Mapping Aquatic and Agricultural Vegetation of Altiplano Using Spaceborne Radar Imagery

Roberto Quiroz[1] and Sassan Saatchi[2]

1. Centro Internacional De La Papa (CIP)
Apartado 1558
Lima, Peru
2. Jet Propulsion Laboratory
4800 Oak Grove Drive
Pasadena, California 91109

Abstract

In this paper, a detailed analysis of L-band and C-band multipolarization spaceborne radar data for classification of agricultural and aquatic vegetation is performed. The study area is around Lake Titicaca, in the high plateau of Altiplano in the Andes, between Bolivia and Peru. The terrain is fragmented to small size cultivated land parcels with rudimentary farming technology and high variability in growth due to the crop rotation patterns practiced in the region. The SIR-C data acquired in April of 1994, field observation and ground data are used to classify the images into land cover types. The analysis includes, a test of separability of classes using data extracted from training areas, the use of a linear discriminant function to classify the training sites, application of principal component on SIR- C channels, and explanation of results based on the sensitivity of radar data at each channel to vegetation biomass and structure and underlying soil condition.
The classification is performed by a maximum likelihood classifier and the accuracy is measured over training and independent test sites and expressed in terms of confusion matrix. The combination of both frequencies and polarization channels resulted in less than 10% error both on training and test sites. It is shown that current single channel spaceborne radar systems such as JERS-1 and Radarsat produce more than 40% error (20% when combined). This result indicates that the cross-polarization channels in C-band and L-band are important to identify vegetation structure and type.

INTRODUCTION

The high plateau or Altiplano, is made up of a series of plains, highlands, and isolated hills, situated in the Andes from about 14° to 22° south latitude, between Bolivia and Peru, at an elevation of more than 3,600 meters above the sea level. It is home to more than 2 million people, distributed approximately equally between Peru and Bolivia (GS/OAS, 1996). The main areas of cultivation are on the level ground and gentle hills bordering Lake Titicaca. By and large, these are the most densely populated rural areas, characterized by highly fragmented terrain with many parcels of land of uneconomic size, high levels of poverty and low yields, attributable primarily to rudimentary farming technology. Nevertheless, it is the output of these areas that is intended in large part for national consumption in both countries . The main crops throughout the Altiplano are potato, quinoa, oat, and barley. Cultivated and native pastures are also widespread throughout the area (Quiroz et al., 1997).

Availability of data on actual land use is crucial for appropriate decision making on land use development and research targeting. The demand for actual and potential land uses is increasing with the decentralization of the planning of rural development actions to and the implementation by the local governments. Land use data for the Altiplano is scarce, probably because of the high costs associated with data gathering and processing, when conventional methods are used (e.g. transect evaluation, airphoto interpretation, thematic cartography, etc.). This is of particular importance because the large spatial variability in land use/cover demands a larger sample size to produce accurate land use land cover maps. The lake vegetation, required to maintain the diversity of fishes and birds which also constitute the best quality forage for feeding beef/dairy animals in the area, is not adequately mapped nor a cost effective way to monitor their changes in time has been proven.

Fine and course resolution optical imagery, such as Landsat-TM and AVHRR, are being used to elaborate land use maps and to monitor land use/land cover changes. Despite the effort, the accuracy of the outputs varies, particularly during the cropping season, in the areas of cultivation. Several reasons contribute to this lack of accuracy, being of most importance: (1) the area is continuously covered with clouds during the cropping period, which coincides with the rainy season; (2) the small size of the crop plots which combined with the rotation pattern of crops and pasture generates large variability over small areas; and, (3) the similarity of the land cover types in growth habits, growth and development patterns, and canopy architecture. Some of the limitations for the successful use of optical remote sensing in the Altiplano can be circumvented by spaceborne radar data, particularly

because their insensitivity to cloud cover and the capability to penetrate the vegetation layer (Foody, 1994; Saatchi, 1996).

The objective of this paper is to demonstrate the potential use of spaceborne polarimetric radar in mapping land cover and land use in the Altiplano. SIR-C L- and C-band data acquired in April of 1994 over Lake Titicaca between Huarina and Jesus de Machaca in the Department of La Paz, was used for this study. The paper describes the most important land cover types in the cultivation area of the Altiplano as well as the aquatic vegetation in the lake, and the application of a maximum likelihood Baysian procedure to classify land cover types with canopy similarities. Several studies in recent years have addressed the use of radar data for land cover classification in a variety of landscapes such as cultivated areas (Foody et al., 1994), boreal and temperate forests (Rignot et al., 1994; Saatchi and Rignot, 1996), tropical forests (Saatchi et al., 1997; Rignot et al., 1997), and wetland and coastal areas (Hess et al., 1995; Pope et al., 1994). In most of these studies, classification have been performed using standard methods in order to demonstrate the readily applicability of the SAR data in land cover classification.

In this paper, we also examine standard methods to classify the SIR-C images. We compare the advantages of using intensity, amplitude, backscattering, or digital numbers data. The usefulness of applying principal component transformation to gain insight on the data structure and to improve the classification accuracy is discussed as well. In the following sections, the study area, the characteristics of SIR-C image data, the characteristic of land cover types in the region under investigation and the data analysis and classification are discussed.

STUDY AREA

The area Huarina Desaguadero was chosen because it is highly representative of all the agricultural land under the influence of Lake Titicaca (Figure 1). It encompasses zones in the lake with abundance of aquatic vegetation. It also contains cropping land at both, level ground and hillsides. Rangelands are ubiquitous and grazing marsh are common. Due to the prevalence of dairy in the area, alfalfa is becoming an important crop. Eucalyptus trees and other shrubs (e.g. tola) are scattered all over the area with a few spots with more dense forested land. Annual rainfall ranges from 700 mm to 800 mm. The seasonal distribution of the rain is similar throughout the region - typically monomodal, with a rainy season from December to March and a dry period from May to August. Annual rainfall fluctuates more than 50% from the mean.

Mean annual temperatures range from 8° to 10° C, the highest occurring from December to March. The minimum mean monthly temperatures is approximately -7° C.

Winds are predominantly calm, although velocities of up to 4 and 5 m/s have been recorded in the Lake Titicaca zone and the eastern area, respectively. Evaporation is very high, reaching annual means of 1,450 mm near and at Lake Titicaca. The evapotranspiration potential varies from 1,000 to 1,500 mm over the region, with the highest values occurring from November to March and the lowest from May to August. According to the Thornthwaite climate classification, most of the study area is characterized by rainy or semi-rainy and cold climates, and a small portion to the south, has a semiarid cold climate (GS/OAS, 1996).

Because of the altitude and low temperatures, most of the soils are deficient in organic material and nitrogen and therefore require special measures to maintain and increase their productivity. In the non-arable part, terracing systems dating back to pre-Columbian civilizations survive on the hillsides. These lands include eolian accumulations, slope deposits, marshes in the middle and upper basins, and the dissected volcanic meseta. Abundant stones created by glacial activity limit their use to controlled forestry and grazing of camelides or sheep, especially in the marshes (GS/OAS,1996).

Comparing the potential with the actual use of the soils shows that at least a third of the lands are being overused. This overuse occurs especially on marginal land and land suited neither to annual, continuing cultivation nor to controlled silvopastoral uses.

The loss of farmland is due mainly to erosion and salinization. It has been estimated that 30% of the soils show severe and very severe erosion resulting from present and past farming and grazing activities and hastened by the System's geological conditions. In fact, the most serious problems have developed on gently and steeply sloping hilly land, terraces and mesetas. In some specific situations erosion may be related more to natural geological evolution than to land use.

Within this general system, the special conditions created by Lake Titicaca and other lakes of the Altiplano have given rise to a unique aquatic vegetation, among which the reed banks (totora) are particularly important both ecologically and economically. The lakes provide habitats for a great variety of aquatic birds, many of them migratory, and some native fishes that still retain a certain commercial importance.

Practically the entire Altiplano is a single natural grassland, varying in aspect according to climate and soil. It is richest in forage in the marshy areas, which yield more than 2,500 kg of dry matter (dm) per hectare and year. The productivity of meadows where grasses predominate ranges from 1,000 to 1,600 kg, although on some types of scrubland that figure drops to between 130 and 210 kg. The productivity of scrubby or grass-and-shrub meadows is also very low: some 150 to 210 kg dm/ha. Consequently, the animal-carrying capacity varies greatly.

Shuttle Imaging Radar Data

SIR-C/X-SAR shuttle mission is a cooperative experiment among NASA, the German Space Agency and the Italian Space Agency and was launched on space shuttle Endeavor on September 30, 1994 for a 10 day mission. This was the second deployment of the SIR-C instrument (the first was launched April 9, 1994). Both the SIR-C instrument and ground data processor were developed by NASA's Jet Propulsion Laboratory.

SIR-C provides increased capability over earlier orbital radar systems such as Seasat, SIR-A, and SIR-B, and the European ERS-1 and Japanese JERS-1, by acquiring digital images simultaneously at two microwave wavelengths, L-band (λ=24 cm) and C-band (λ=6 cm) (13) . The system is fully polarimetric, having the capability to transmit and receive horizontal (H) and vertical (V) polarization on separate channels. In addition to the SIR-C instrument, the X-SAR system operates at X-band (λ=3 cm) with only VV polarization (transmit vertical and receive vertical).

The data acquired over the Altiplano by the shuttle imaging radar SIR-C/X-SAR in April of 1994 are shown in figure 2. This image is a color composite of three bands, made by assigning red to L-band HH, green to L-band HV, and blue to C-band HH polarizations. The colors in the image indicate relative intensity of the backscatter power received from the unit ground resolution cell in the imaged scene (backscattered coefficient). The backscattered coefficient is analogous to the optical reflectance measured by optical sensors such as the Landsat Thematic Mapper in that it is a dimensionless quantity characteristic of the scattering behavior of the elements in the ground resolution cell. The resolution of the image is approximately 25 meters.

The unique attribute of multiwavelength polarimetric radar analysis is that the penetration depth of the signal provides information on the presence of canopy components such as leaves, branches, and trunks as a function of wavelength. Longer wavelengths penetrate more deeply because they interact less with small scale canopy elements such as leaves and small branches. Over low vegetated areas such as grasslands, crops, and aquatic vegetation, data from both wavelengths interact with the underlying soil or water and add useful information that can be used for classification. The multiwavelength and polarimetric configuration of the SIR-C/X-SAR system can thus provide information about the structure, biomass, and underlying soil moisture and water over vegetated landscapes unavailable in or different from any other remote sensing data.

LAND COVER TYPES

Three categories of land-cover types were studied: 1)aquatic vegetation, 2) land vegetation, and 3) villages. The multilevel classification system based on remote sensing

(Anderson et al., 1976; Sabins, 1997) was used to select the classes. A more detailed description follows.

Aquatic Vegetation

The aquatic vegetation is composed of plankton and macrophytes. They correspond to submerge aquatic vegetation and thus classified in the category 500 (water). Within the macrophytes, there are about 15 species, being the most important ones the llachu (*Elodea potamogeton, myriophyllum elatinoides*), and the totora (*Schoenoplectus tatora*). Macrophytes, particularly llachu and totora, occupy the shallow sector of the lake to up to 15 m deep (Collot, 1980). Llachu and totora constitute the best quality forage available to feed milk/beef cattle in the zone, with digestibility above 65 % and protein contents above 10 % (Quiroz et al., 1997). Totora is also used for roofing and for the construction of reed boats. The association of llachu and totora is also of crucial importance for the subsistence of native fishes and for the nesting of birds. Some of the characteristics that allows the separation of this two types of plants with SIR-C data include: the difference in size providing differentiated backscattering signals in L- and C-bands, the presence of a water mirror underneath the totora thus increasing the double-bouncing backscattering, and the intermingled array presented by totora which enhances the volume backscattering.

Land Vegetation

The agricultural zone was classified as cropland and pasture (210). This level II category included potato, barley, oat, alfalfa, and quinoa, all cultivated in small plots. The crop rotation head is potato, followed by any of the cereal crops for the next two to three years. In recent years, farmers near the lake are introducing broad beans in the fourth year. The fallow period varies between one to four years, as a function of both the farm and the family sizes. Most of the plots close to the lake are under continuous cropping. During the fallow years, native vegetation grows and the area is grazed. With the implementation of dairy policies for the Altiplano, by the late eighties, the area cropped with alfalfa has grown substantially.

Rangelands(300) constitute by far the main land cover in the Altiplano. Rangelands were divided into two main land cover types, conforming to the classes 310 and 330 of level II; grasslands and mixed rangelands, respectively. Grasslands are composed of different associations of plant species - of different size, density, growth habits, and canopy architecture - according to precipitation, soil type, and altitude, among other factors.

Mixed rangelands are presented as patches all over the study area. It is an intermixture of grassland with shrub and brushland, and in some instances with scattered trees. The most abundant tree specie is eucalyptus. Growth and development of eucalyptus in the Altiplano is very slow, due to the adversity of the environment such as constant frost and prolonged period without precipitation. Their thin trunks and scarce canopy resemble more to shrubs than to forest. Other types of vegetation in this class included *Polylepis*, *Chuquiraga*, *Parasthrephya*, and *Baccharis*, commonly known as queñoa, kisuara and tola (the latter 2 species), respectively. In the zones near the lake, the yellow or inland totora is also considered in this class.

Bofedales, grazing zones in water logged tracts, were delimited as herbaceous vegetation-class 621 of level III, a subdivision of vegetated wetlands nonforested (620). They could be permanent, receiving constant inflow of water throughout the year or temporal (around 6 months a year) humid depressions. They are characterized by a rich flora of good quality, of vital importance for the production of camelides. Since bofedales are the only source of pasture for grazing animals lasting year-round, they are usually heavily grazed. Another particularity of bofedales is the roughness of the terrain produced by the erosion of the soil if the water is not managed correctly, the trampling by the animals, and the occurrence of patches of grasses particularly in temporal bofedales. The high density of plants per area, the high water content, and the low size of the plants differentiate the backscattering characteristics of these plants from other grasslands.

Villages

Several towns and villages are contained in the images. The most important towns are: Huatajata, Huarina, Batallas, Puerto Perez, and Guaqui. Small villages and scattered farmer's houses are spread all over the image. Because of the size of the towns and villages, it is difficult to separate other urban or built-up level II classes and was then classified as mixed built-up (180) category (Sabins, 1997). This class is easily separated from other land-cover types, due to its high backscatter signals. The areas with pronounced topography also present backscattering values similar to those of buildings and houses and therefore produces a misclassification of these pixels.

CLASSIFICATION METHODOLOGY

The first step consisted of the definition of the ground cover types. As explained above, the eight cover types selected were: llachu, totora, crops/pasture, grasslands, mixed rangelands, bofedal, and villages. Twenty five training sites were chosen for each of the eight land-cover types described above. A training site was composed of a window of 3

pixels by 3 pixels, of the most representative areas of each land-cover type throughout the image. A 3X3 window was selected to cover an area that would be large enough to represent a given class, and at the same time sufficiently small to minimize the possible effect of the existing spatial variability. The spatial variability can be attributed to several reasons including: the atomization of land ownership in the lake-shore, the crop rotation pattern in these small plots, and the topography of the terrain. The effect of the topography was not corrected for, due to the lack of a high resolution digital elevation model.

The training data was used to estimate the parameters of the classifier algorithm, and to assess the accuracy of the classification of the automated process over the entire image. A supervised classification of the SIR-C data was performed using a maximum likelihood Baysian method. The prior probability was calculated as the ratio between the number of observations corresponding to each land cover type and the total number of observations in the training sites.

A validation of the estimated parameters of the classifier was executed on 11 test sites independently chosen. Land-cover types were classified using the discriminant function developed with the data from the training sites. The classification accuracy was then used as the estimator of the accuracy of the automated process when the maximum likelihood estimator is used. The classification of land-cover types for both training and test sites was run on amplitude, intensity, backscattering, and digital numbers data.

The learning procedure for the classifier is supervise in the sense that the class labels are known in advance and training areas are chosen on the basis of visual interpretation of the image, aided by a good knowledge of the area, plus field data. Because the SIR-C radar data used in this study were acquired in mode 11 with only two polarization to accommodate for wider swath, the polarimetric classifier has been modified to work with the individual channels instead of the full polarimetric covariance matrix.

The data contained in any pixel of a radar imagery, for different channels, is derived from the response of the same backscatterers. Consequently, one expects an interdependent response. In the case of SIR-C, mode 11, it implies that a linear dependency among the four channels (LHH, LHV, CHH, CHV) might exist, and thus a multicollinearity problem. In which case, the actual multidimensional space described by the recorded responses in the channels is smaller than the multidimensional space defined by the four bands, if they were totally independent. This repetition of information might be a source of noise thus creating potential problems in the classification of the image. The singular value decomposition of the backscattering matrix was performed to look at the structure of the variability and to evaluate its usefulness in the classification of the defined land-cover types. The same

maximum likelihood procedure described above was used on the image filtered through this principal component decomposition of the covariance matrix.

RESULTS AND DISCUSSION

Most routine automated classifications are performed using digital number imagery. In this study we aimed at determining the appropriateness of using DN imageries and at the same time, to quantify the differences in the accuracy of classification for the eight selected land-cover types, as a function of the type of data used to estimate the discriminant function. Amplitude, intensity, backscattering in dB, and digital numbers data were compared. Table 1 summarizes the results.

The multidimensional dynamic range of the intensity data proved to be the smallest, thus decreasing the separability among the land-cover types. The overall accuracy of classification was 64 %. In the case of amplitude, the overall accuracy increased to 80%. There was no difference whatsoever in using digital numbers or backscattering dB values. The accuracy in this case was the highest, being 94 %. The discussion below is then focused on the discrimination of land-cover types, based on backscattering values.

Backscatter Data For Training Sites

The backscatter characteristics of the training areas (Table 2) were used to create the first land-cover classification. All four channels of the SIR-C data (LHH, LHV, CHH, and CHV), were used to produce the classification, because theoretically, inclusion of all available polarimetric channels should yield the highest accuracy.

A simple inspection of the table provides some insights on some of the attributes of the land-cover types. The high water content of the aquatic plants (up to 90 %) is shown in the strong backscattering. Totora, with mature height of more than a meter, was brighter at all four channels used. The smaller llachu (a few centimeters above the water level), is bright only at C-band. Grasslands produce consistently low backscattering in all four channels. Mixed rangelands differ from grasslands in the strong response in the like-polarized L-band, evidencing the presence of taller vegetation. These vegetation show relatively weak volume scattering , associated with low density canopy of shrubs, small trees and/or tall grasses. Crop and pasture plants, such as alfalfa, are expected to have higher water content than the grasses in the grasslands or mixed rangelands, and thus a higher dielectric constant. This might be the reason why the returned energy for crops/pasture was higher than for grasslands, in all four channels. Plants in the bofedal are short and contain a high level of humidity (up to 70 %). This combined with the roughness of the terrain and a high soil moisture, account for the response mainly in the C-band. The

villages show higher values in all four channels. This relative high return signal is due to the geometric characteristics of the buildings combined with the energy return of metal roofing.

Separability

The vector-based measures considering the means and variances of a pair of probability distributions, are referred to as measures of separability. The measures of separability imply the ease with which patterns can be correctly associated with their classes using statistical pattern classification (Richards, 1993).

The pairwise generalized squared distances between land-cover types, a measure of the average distance between the two class density functions, were estimated as:

$$d^2(i,j) = (X_i - X_j)^T \Sigma^{-1} (X_i - X_j) - 2 \ln P_j \qquad (1)$$

Where $d^2(i,j)$ is the squared distance between land-cover classes i and j, X_i is the mean vector of class i, Σ is the covariance matrix, P_j is the a *priori* probability for class j, and ln is the natural logarithm. Table 3 shows the pairwise squared distances among the eight land cover types. The response variable presented is based on backscattering values (dB). The distance within the same class (intraclass) is given by the prior probability (main diagonal). By definition, the prior probabilities are the probabilities with which class membership of a pixel could be guessed before classification. Using these probabilities as a yardstick to compare with interclass distances, we find interclass distances ranging from 3 to 63 times the intraclass distance. The classes with shorter square distances among them are: llachu and bofedal, totora and crops, crops and mixed rangelands, and grasslands and mixed rangelands.

The minimum distance classifier requires a discriminant function. When the distribution within each group is assumed to be multivariate normal, a parametric method can be used to develop a discriminant function (a classification criterion) which is determined by a measure of generalized squared distance (Rao, 1973). The classification criterion can be based on either the individual within-group covariance matrices (yielding a quadratic function) or the pooled covariance matrix (yielding a linear function); it also takes into account the prior probabilities of the groups. A linear discriminant function (equation 2) was used in the present study to classify the eight land-cover types (Table 4).

$$\text{Constant} = -0.5X_j^T\Sigma^{-1}X_j + \ln P_j \; ; \quad \text{Coefficient Vector} = \Sigma^{-1}X_j \tag{2}$$

The difference in magnitude shown for the constant values of each land-cover type suggests that the classes might be well separated. It is also notable that the cross-polarized bands contribute more to the discrimination than the like-polarized bands.

The classification of each observation (pixel) as a land-cover type was based on the calculation of its generalized squared distance (equation 3) and the corresponding posterior probability (equation 4) of that observation in each land-cover type. The observation is then classified in the land-cover type with the highest posterior probability.

$$d_j^2(X) = (X - X_j)^T\Sigma^{-1}(X - X_j) - 2\ln P_j \tag{3}$$

$$P(j \mid X) = \frac{\exp\left[-0.5d_j^2(X)\right]}{\sum_k \exp\left[-0.5d_k^2(X)\right]} \tag{4}$$

Where $d_j^2(X)$ is the distance between the pixel at location X and the centroid of the class, $P(j|X)$ is the probability that a pixel at a location X belongs to a class , and k is all other classes except class j.

The classification accuracy for each class is determined by the ratio between the number of pixels correctly classified into the class and the total number of pixels in that class. The resulting confusion matrix (Table 5) shows an overall accuracy of 94 %. The largest error rates were shown by the misclassification of 16 % of the llachu as bofedal and 12 % of the mixed rangelands pixels as grasslands. Low density llachu have a similar roughness and dielectric constant than bofedal, showing similar cross-polarized C-band signal. For the case of mixed rangelands, when grasses dominate a particular pixel, these class becomes similar to a grassland and can be classified as such.

The discriminant linear function derived with data from the training sites, was used to classify the land-cover types of the testing sites. The confusion matrix of the validation of the classification procedure is shown in table 6. The overall accuracy was also 88%.

Aquatic Vegetation

The accuracy of aquatic vegetation classification was 8%. The confusion matrices from both training and testing sites show misclassification of aquatic vegetation as land vegetation and vice versa. From the interpretation point of view, this is not a major classification problem, since the classification of the aquatic vegetation is only interpreted within water bodies.

The discrimination between llachu and totora, based on the analysis of the radar backscatter signature is depicted in figure 3. All panels in figure 3 show a good separation of the species. The small portion of the llachu canopy above the water surface is small thus presenting a weak return in both LHV and LHH channels. Totora show a higher LHV return mainly because of the dense intermingled array of the reeds above the water level. The strong LHH return correspond to the double-bounce scattering, enhanced by the presence of a water mirror underneath.

Totorales are characterized by having a dense population of reeds and are usually mixed with llachu. That might be the reason why the volume scatter response in the CHV channel was higher than in Llachu alone. Totora also show a higher CHH return. It is interesting to note the wide dynamic range of both CHH and CHV values for totora and llachu. This feature reflects the heterogeneity of mixtures encountered in the lake, where the two types of plants can either exist as pure stands or as mixtures with varied proportions. The backscattering reported for totora in CHH is similar to the values reported by Moreau et al., 1997, working on the same area with Radarsat data.

Land Vegetation

The accuracy of classification within this category was 94 %. The bivariate plots (Figure 4) portray the level of usefulness of the combination of paired channels to discriminate among land-cover classes.

Crops and pasture in this area of the Altiplano consist mainly of potato, cereal crops (barley, oat, quinoa), and alfalfa. The image used was taken in mid April, which coincides with the harvest period. This implies that backscattering mainly from the surface of the cropping areas and the response to the crop residue remaining in the fields, which still contain 20 to 30 % of water, depending on rains, and the alfalfa fields which are still green. Ninety five percent of the training pixels of the crop cover types were in the ranges of -17.77 to -15.39 dB and -23.5 to -21.6 dB for LHH and LHV, respectively. For C-band, crops showed ranges of -19.9 to -17.02 dB for CHH, and -17.91 to -16.55 dB for CHV.

Both the training and the testing areas for grasslands were selected in the pastoral systems of Jesus de Machaca. This zone is being classified as dry arid puna by GS/OAS

(1996). A low density vegetation with patches of bare soil are typical of this zone. The LHH backscattering (-21.27 to -19.71 dB) then correspond to patches of bunched grasses, locally known as pajonales, and roughness variation. The volume scattering (LHV: -29.70 to -28.18) is associated with patches of tall plants (> 50 cm) of mainly *Festuca*.. The lowest backscattering values of all the land-covers, in the C-band (CHH: -26.01 to -24.40, and CHV: -22.78 to -21.66), was shown by pasture. This is due to areas with smooth ground and low vegetation with small leaves. Some of the volume scattering in the C-band, might also be associated to water from recent rainfall retained in the thatch.

The strong double-bounce scattering (LHH) resulting from the mixed rangelands differentiates this land-cover from the other three classes within the land vegetation. Given that the magnitude of the signal is even stronger than the one for totora, this shows the presence of taller vegetation such as brush, scrubs or trees. The 95 confidence interval of dynamic range of this response is -11.74 to -8.8 dB. Backscattering below this confidence interval might be misclassified as grasslands or crops/pasture. On the other hand, the volume scattering detected in LHV ranges from -23.37 to -21.43 dB. This signature is associated with shrubs, scrubs or trees containing low density of branches and leaves, a characteristic of the eucalyptus trees growing in the Altiplano (above 3800 meters above sea level).

Bofedales are wetlands with low and fast-growing vegetation. This land-cover type is heavily grazed, so it is always low (< 10 cm). The surface is highly irregular with natural irrigation channels and soils highly saturated. In the study site, bofedales are small in size and associated with patches of dry-land pastures or rangelands of good quality, due to the closeness to water and the natural fertilization (manure) by grazing animals. The backscattering signatures in L-band may correspond to both volume scattering (LHV: -33.81 to -32.17 dB) and double-bounce backscattering (LHH: -23.98 to -22.2 dB) of the taller and dense grasses. The CHH surface scattering (-18.72 to -16.34) might be related to the roughness of the land and the volume scattering (CHV: -19.58 to -18.50 dB) can be associated with the short, dense, and high-water-content vegetation typical of this land-cover type.

Moreau et al (1997) reported backscattering values from -13.6 to -9.1 dB, using data from the RADARSAT satellite (CHH). These backscattering values are significantly higher, in both absolute value and range, than the values shown in the present study. This difference can be explained by the different procedures used to select the areas over which the backscattering values were extracted. In the Moreau et al (1997) study, the objective was to estimate the biomass produced in the bofedal area over time. The biomass was estimated over an area of approximately 700m x 700m, and so was the extraction of the

backscattering values. Due to the spatial heterogeneity, the backscattering showed such a variability. In the present study, the extraction of the backscattering value was performed on a window of an approximate size of 75m x 75m. A smaller box size, relative to the scale of the variability, and a larger number of samples explain the variability. The difference may also be due to the different calibration and dynamic range of the Radarsat and SIR-C C-band images.

It is evident from the bivariate plots that no pair of channels can separate all land vegetation classes accurately. Therefore, the information contained in all four channels should be combined. All four channels combined resulted in a good classification (accuracy of 94 %) of the land-cover in this subgroup of land vegetation. As can be seen in figure 4, the combinations among LHH, LHV, and CHH appear to contribute the most to the classification.

Villages

This is a stand-alone class. The corner reflector effect and the metal roofing, of both urban areas and the houses in the widespread presence of communities, are clearly distinguishable in all four channels of SAR data.

Classification With Different Combination of Channels

Table 7 shows the error rate of the classification of the eight land-cover types, using different combination of channels. It is important to note that none of the channel alone is able to perform a good classification. Like-polarized L-band seems to be the best single channel to classify the land-cover types encountered in the Altiplano. Channels LHH and CHH were used to simulate a classification of data from JERS-1 or RADARSAT satellites. Based on these results, neither of the two sources of radar data produces a good classification of the most important land-cover types in the Altiplano. By combining the LHH and CHH bands, the accuracy of classification increased to around 86 %. Combination of data from these two satellites is thus recommended. Figure 5 shows the classified map of the SIR-C data using all four channels. The classification is performed by a supervised maximum likelihood classifier using the training data as described earlier.

Principal Component Analysis

The principal component analysis was performed on the variance-covariance matrix of the backscattering signatures in the four channels (LHH, LHV, CHH, CHV). As shown in table 8, the first principal component, associated with the combination of the two

channels in the L-band, and the CHH band contains 80 % of the total variability. The addition of the second principal component, corresponding to the channel CHH, adds 17 % of the total variability. The third principal component is bipolar with a strong additional contribution from CHV. The three principal components combined add up to 99 % of the total variability.

The same procedure described above for the classification of land-cover types, based on backscattering, was followed using the principal components. The classification produced with the principal component did not differ from the one using the backscattering signatures (Figure 6.) The results for the aquatic vegetation is not shown, due to the similarity with the scatter plot of backscattering signatures. The use of two or more principal components to classify the land-cover types produces acceptable to good results (Table 9). The classification accuracy with three principal components was comparable to that obtained with the four channels. The use of two principal components produced better classification than the ones obtained with any combination of two channels and a comparable accuracy with the one produced using the two L-bands plus CHV band.

SUMMARY AND CONCLUSION

In this paper, the application of spaceborne radar imagery for mapping aquatic and agricultural vegetation in high altitudes of the region of Altiplano was studied. It was shown that a combination of C-band and L-band radar data can successfully discriminate several types of vegetation cover types in the region. This result was obtained by examining standard classification methodologies such as principle component analysis, minimum distance classifier, and separability tests. The wide dynamic range of SIR-C data (about 40 dB) was important to separate low vegetation cover types. The aquatic vegetation showed distinguished signatures both at L-band and C-band due to the underlying water surface and the double bounce feature in co-polarized channels and volume scattering in cross-polarized channels. The best accuracy (about 95%) was found when all band and polarizations were combined. The presence of cross-polarized channels were crucial in separating vegetation with various density or biomass levels. As in the case of current spaceborne radar systems, the combination of CHH channel of Radarsat and LHH of JERS-1 showed lower accuracy (about 85%). As radar data from future systems such as LightSAR (L-band polarimetric) or Envisat (dual channel C-band) become available, monitoring the such high altitude ecosystems with continuous cloud cover become feasible. Future studies include the use of multitemporal data for discriminating annual and perennial crops and regions under permafrost conditions.

Acknowledgment

This work was performed during the Sabbatical visit of R. Quiroz at the Jet Propulsion Laboratory in 1998. The funding during this period was provided by Centro Internacional de la Papa (CIP). The work by S. Saatchi was performed at the Jet Propulsion Laboratory, California Institute of Technology under a grand from National Aeronautics and Space Administration.

REFERENCES

Anderson, J.R., Hardy, E.T., Roach, J.T., and Witmer, R.E. 1976. A Land use and land cover classification system for use with remote sensor data: U.S. Geological Survey Professional Paper 964.

Collot, D. D. 1982. Mapa de la vegetación de la bahía de Puno. Ecología en Bolivia 2:49-63.

Foody, G.M., and Curran, P.J., 1994, Estimation of tropical forest extend and regenerative stage using remotely sensed data, *J. of Biogeograhy.* 21:223-244.

General Secretariat of the Organization of American States (GS/OAS) 1996. Diagnóstico Ambiental del Sistema Titicaca-Desagudero-Poopó-Salar de Coipasa (Sistema TDPS) Bolivia-Peru. Washington D.C. 192p.

Hess, L.L., Melack, J.M., Filoso, S., and Wang. Y., 1995, Delineation of inundated area and vegetation along the Amazon floodplain with the SIR-C synthetic aperture radar, *IEEE, Trans. Geosci. Remote Sens.*, vol. 33, 896-905.

Moreau, S., Le Toan, T., Quiroz, R., and Rosich Tell, B. 1997. Quantification of soil moisture and biomass of native forages in the northern Bolivian Altiplano through C-Band SAR data. Sociedad de Especialistas en teledetección y Sistemas de Información Espacial (SELPER). Venezuela.

Pope, K.O., Rey-Benayas, J.M., and Paris, J.F., 1994, Radar remote sensing of forest and wetland ecosystems in the Central American tropics, *Remote Sens. Environ.* vol. 48, 205-219.

Quiroz, R., Pezo, D., Rearte, D., and San Martin, F. 1997. Dynamics of feed resources in mixed farming systems in Latin America. In: C. Renard (Ed). Crop Residues in Mixed Crop/Livestock Farming Systems. CAB International, London UK, pp 149 - 180.

Rao, C.R. (1973). *Linear Statistical Inference and Its Application.* Second Edition. John Wiley & Sons, Inc. New York.

Richards, J. A. 1993. *Remote Sensing Digital Image Analysis: An Introduction*, Springer-Verlag. Berlin.

Rignot, E., Williams, C., Way, J., and Viereck, L.A., (1994), Mapping of forest types in Alaskan boreal forest using SAR imagery, *IEEE Trans. Geosci. remote Sens.* 32:1051-1059.

Rignot, E., Salas, W., and Skole, D.L, 1997, Mapping deforestation and secondary growth in Rondonia, Brazil, using imaging radar and thematic mapper data, *Remote Sens. Environ.*, 59:167-179.

Saatchi, S.S., Soares, J.V., and Alves, D.S., 1997, Mapping deforestation and land use in Amazon rainforest using SIR-C imagery, *Remote Sens. Environ.*, vol. 59, 191-202.

Saatchi, S.S., and Rignot, E., 1996, Classification of boreal forest cover types using SAR images, *Remote Sens. Environ.* 60:270-281.

Sabins, F. F. 1997. *Remote Sensing: Principles and Interpretation*, Third edition. W.H. Freeman and Company. NY.

FIGURE CAPTION

Figure 1. Map of the Altiplano within Peru and Bolivia showing the study area.

Figure 2. SIR-C color composite image of part of the Altiplano. The RGB channels are LHH, CHV, and CHH.

Figure 3. Separability of aquatic vegetation based on bivariate analysis of radar backscatter signals.

Figure 4. Separability of vegetation types based on bivariate analysis of radar backscatter data.

Figure 5. Map of land-cover classes obtained by using LHH, LHV, CHV, and CHH channels of SIR-C data.

Figure 6. Separability of vegetation types based on PCA of radar backscatter signals.

Table 1. Percent error in classifying land cover types over different types of radar data.

Data Source	Llachu	Totora	Crops	Grassland	Mixed Rangeland	Bofedal	Village	Total Error
Amplitude	11	12	20	0	28	8	0	11
Intensity	48	20	28	0	28	12	4	20
dB/DN	8	4	8	0	12	4	0	5

Table 2. Backscatter Statistics (dB) of Training Sites for Land-Cover Type Classes at L-Band and C-Band Frequencies

Class	σ^0, HH	Sx	σ^0, HV	Sx
L-Band				
Water	-33.00	1.00	-38.61	0.38
Llachu	-25.37	0.40	-36.49	0.37
Totora	-11.98	0.39	-21.67	0.32
Crops	-16.58	0.58	-22.55	0.46
Grasslands	-20.49	0.38	-28.94	0.37
Mixed rangelands	- 9.97	0.86	-22.40	0.47
Bofedal	-23.09	0.58	-32.99	0.40
Village	-3.35	0.43	-14.40	0.36
C-Band				
Water	-39.92	0.08	-25.93	0.22
Llachu	-11.18	0.55	-18.69	0.37
Totora	-10.52	0.87	-14.23	0.31
Crops	-18.46	0.70	-17.23	0.33
Grasslands	-24.40	0.78	-22.22	0.27
Mixed rangelands	-20.00	0.98	-20.37	0.18
Bofedal	-17.53	0.58	-19.04	0.26
Village	-6.85	0.57	-12.43	0.34

Sx =standard error of the mean

Table 3. Generalized Squared Distance Among Land-Cover types.

Class	Llachu	Totora	Crops	Grassland	Mixed Rangeland	Bofedal	Village
Llachu	3.89	64.79	64.95	54.67	97.62	12.46	149.87
Totora	64.79	3.89	13.78	51.48	36.65	42.19	19.97
Crops	64.95	13.78	3.89	23.68	20.61	32.80	38.74
Grassland	54.67	51.48	23.68	3.89	21.64	22.998	99.93
Mixed Rangeland	97.62	36.65	20.61	21.64	3.89	54.06	52.40
Bofedal	12.46	42.19	32.80	22.98	54.06	3.89	105.33
Village	140.87	19.97	38.74	99.93	52.40	105.33	3.89

Table 4. Numerical values of discriminant linear function for classifying land-cover types.

Channels	Llachu	Totora	Crops	Grassland	Mixed Rangeland	Bofedal	Village
Constant	-203.29	-90.03	-115.73	-192.35	-150.98	-183.56	-59.18
LHV	-8.24	-4.99	-4.56	-5.93	-4.99	-7.27	-3.60
LHH	0.29	1.09	0.75	1.15	2.26	0.64	1.78
CHV	-5.63	-5.14	-6.56	-8.52	-8.48	-6.33	-5.10
CHH	-0.35	-0.75	-1.31	-1.78	-1.80	-1.00	-0.76

Table 5. Confusion Matrix of Land-Cover Types in the Training Sites Derived from the Bayesian Classifier. The numbers are in percent and the total error is 5%.

Class	Llachu	Totora	Crops	Grassland	Mixed Rangeland	Bofedal	Village
Llachu	92	0	0	0	0	8	0
Totora	0	96	4	0	0	0	0
Crops	0	8	92	0	0	0	0
Grassland	0	0	0	100	0	0	0
Mixed Rangeland	0	0	0	12	88	0	0
Bofedal	4	0	0	0	0	96	0
Village	0	0	0	0	0	0	100
Error Rate	8	4	8	0	12	4	0

Table 6. Confusion matrix of land cover types in the validation sites derived from the Baysian Cclassifier. Total error is 5%.

Class	Llachu	Totora	Crops	Grassland	Mixed Rangeland	Bofedal	Village
Llachu	91	0	0	0	0	9	0
Totora	0	100	0	0	0	0	0
Crops	0	0	91	0	0	9	0
Grassland	0	0	0	100	0	0	0
Mixed Rangeland	0	0	0	9	82	9	0
Bofedal	9	0	9	0	0	100	0
Village	0	0	0	0	0	0	100
Error Rate	9	0	9	0	18	0	0

Table 7. Classification error rate (%) for land-cover types in the Altiplano using different combination of channels from SIR-C imagery.

Channels	Training Sites	Test Sites
LHV	40.57	45.45
LHV, LHH	27.43	20.78
LHV, LHH, CHV	10.86	9.09
LHV, LHH, CHV, CHH	6.86	5.19
LHH	36.57	44.16
CHH	56.57	46.75
LHH, CHH	17.71	15.58

Table 8. Principal component analysis of the SIR-C radar backscattering signatures.

	Eigenvalue	Difference	Proportion	Cumulative
PRIN1	222.428	176.151	0.801306	0.80131
PRIN2	46.277	40.405	0.166713	0.96802
PRIN3	5.871	2.865	0.021151	0.98917
PRIN4	3.006	.	0.010830	1.00000

Eigenvectors

	PRIN1	PRIN2	PRIN3	PRIN4
LHV	0.485058	0.485776	0.504423	-0.523735
LHH	0.591736	0.412233	-0.591363	0.360836
CHV	0.249227	-0.105424	0.623473	0.733521
CHH	0.593678	-0.763526	-0.084440	-0.239678

Table 9. Classification error rate (%) for land-cover types in the Altiplano using principal components of backscattering signatures.

Principal Component	Training Sites	Test Sites
One Component	37.14	46.75
Two Component	13.14	7.79
Three Component	6.86	6.49
Four Component	6.86	5.19

Figure 1. Map of the Altiplano within Peru and Bolivia showing the study area.

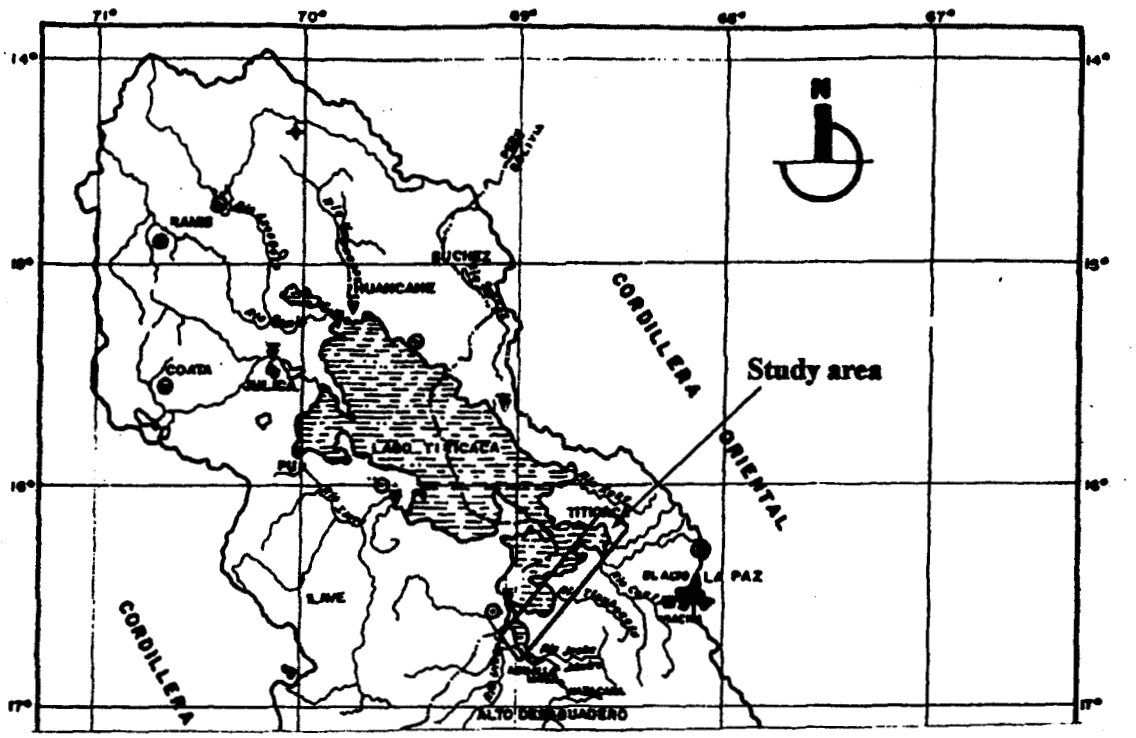

Source: GS/OAS, 1996

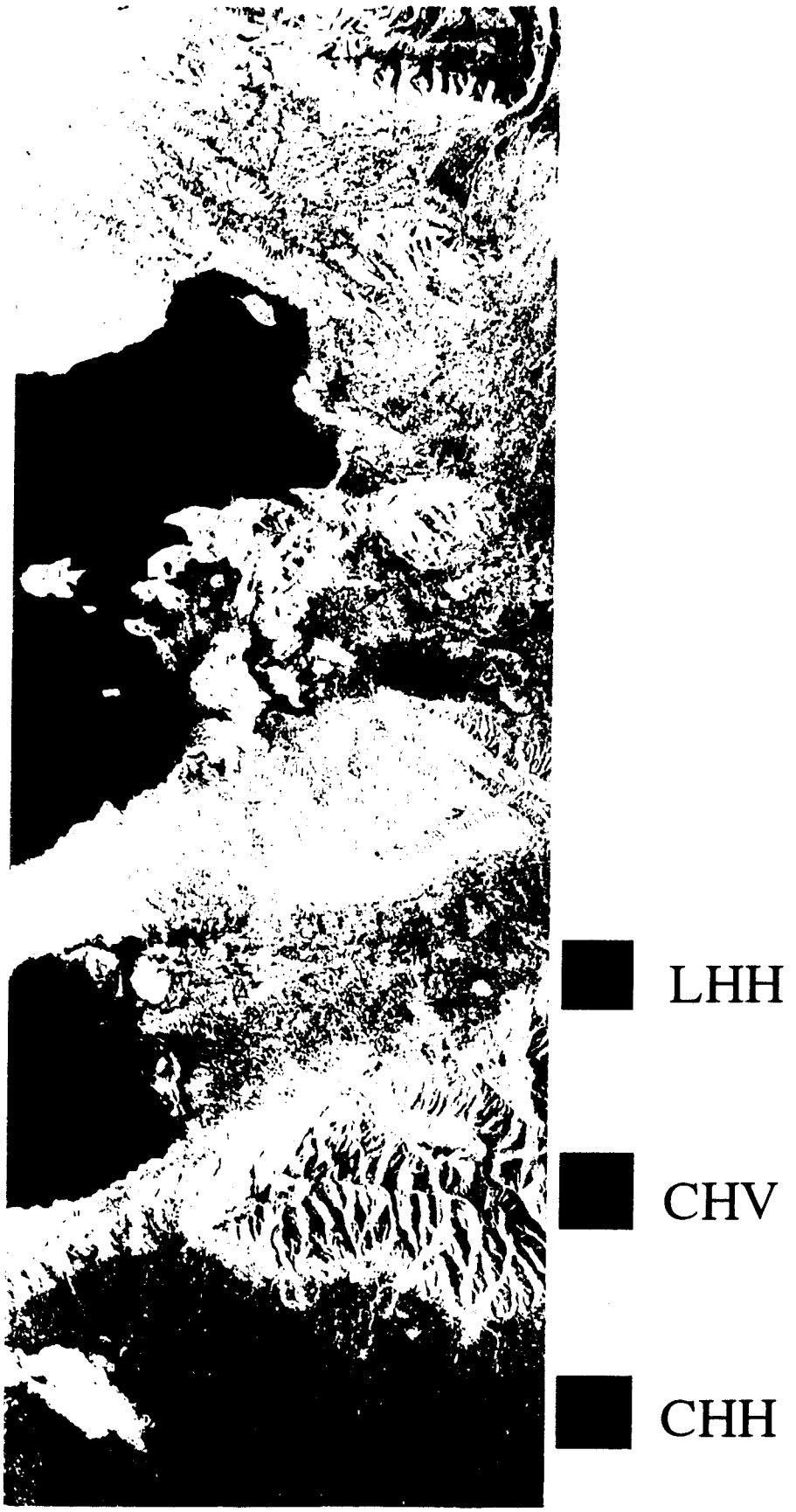
LHH
CHV
CHH

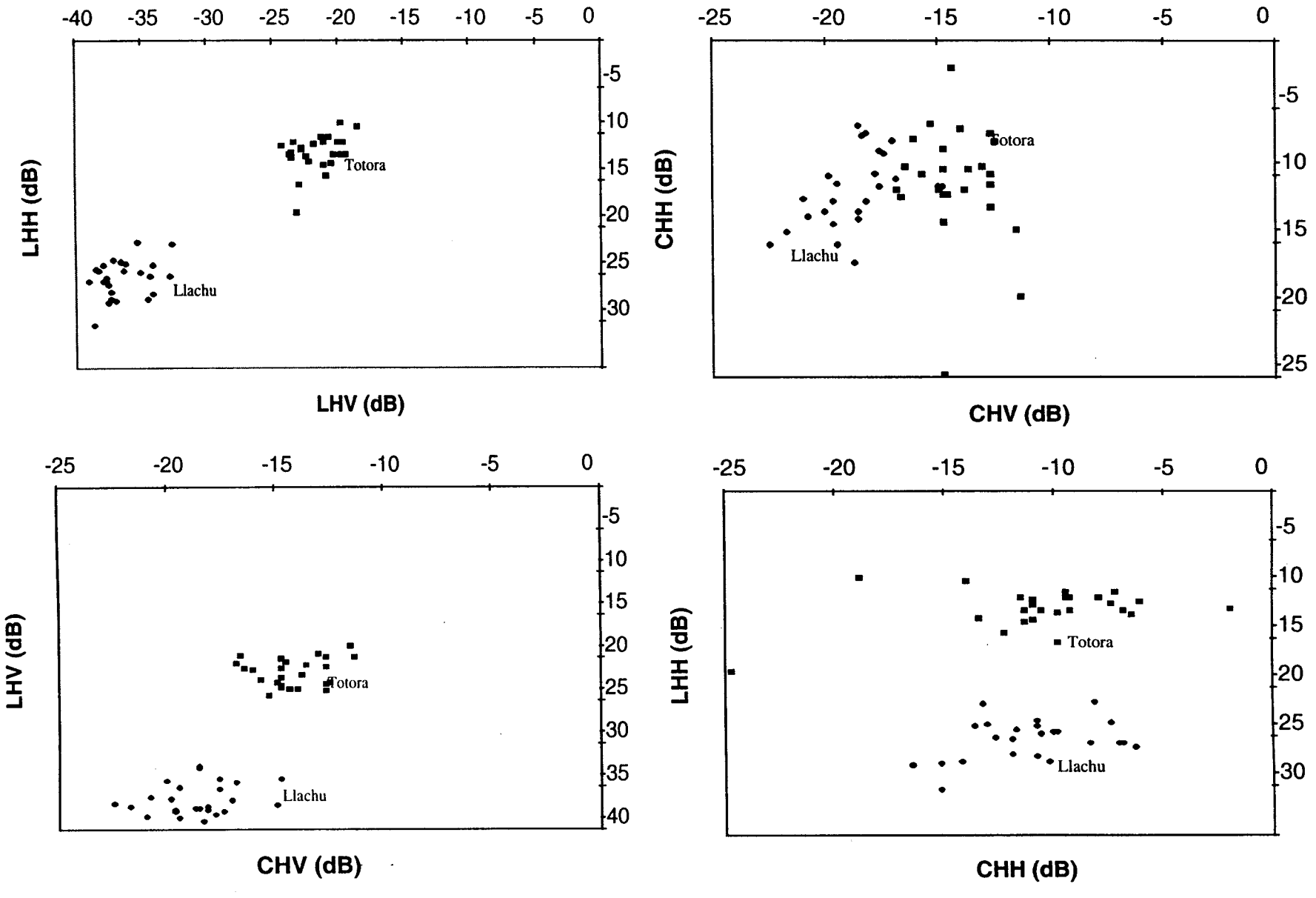
-40 -35 -30 -25 -20 -15 -10 -5 0
-5 10 15 20 25 30
LHH (dB)
Totora
Llachu
LHV (dB)
-25 -20 -15 -10 -5 0
-5 10 15 20 25
CHH (dB)
Totora
Llachu
CHV (dB)
-25 -20 -15 -10 -5 0
-5 10 15 20 25 30 35 40
LHV (dB)
Totora
Llachu
CHV (dB)
-25 -20 -15 -10 -5 0
-5 10 15 20 25 30
LHH (dB)
Totora
Llachu
CHH (dB)

Figure 3.

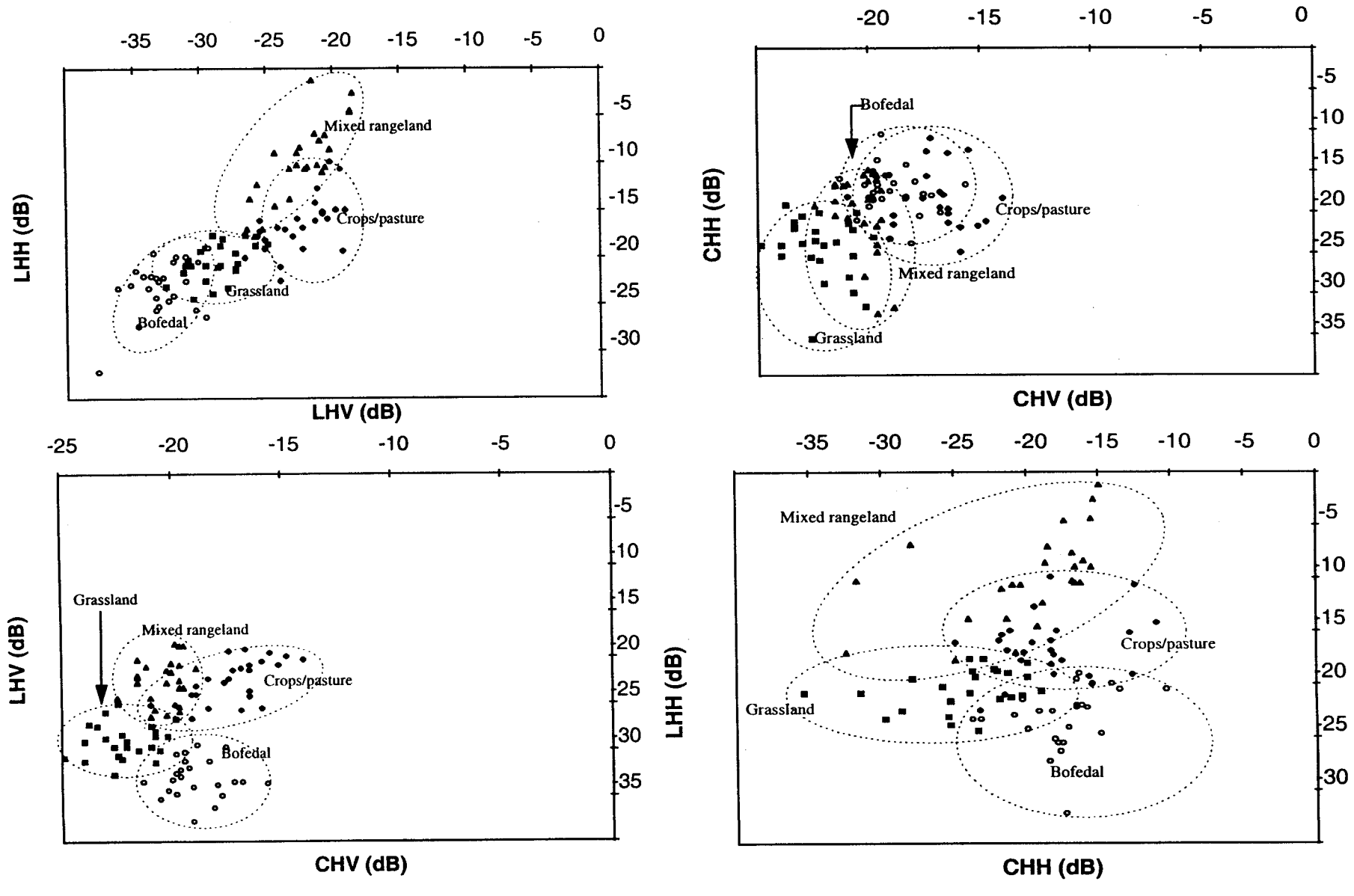
-35 -30 -25 -20 -15 -10 -5 0
-5 -10 -15 -20 -25 -30
LHH (dB)
LHV (dB)
Mixed rangeland
Crops/pasture
Grassland
Bofedal
-20 -15 -10 -5 0
-5 10 15 20 25 30 35
CHH (dB)
CHV (dB)
Bofedal
Crops/pasture
Mixed rangeland
Grassland
-25 -20 -15 -10 -5 0
-5 10 15 20 25 30 35
LHV (dB)
CHV (dB)
Grassland
Mixed rangeland
Crops/pasture
Bofedal
-35 -30 -25 -20 -15 -10 -5 0
-5 10 15 20 25 30
LHH (dB)
CHH (dB)
Mixed rangeland
Crops/pasture
Grassland
Bofedal

Figure 4.

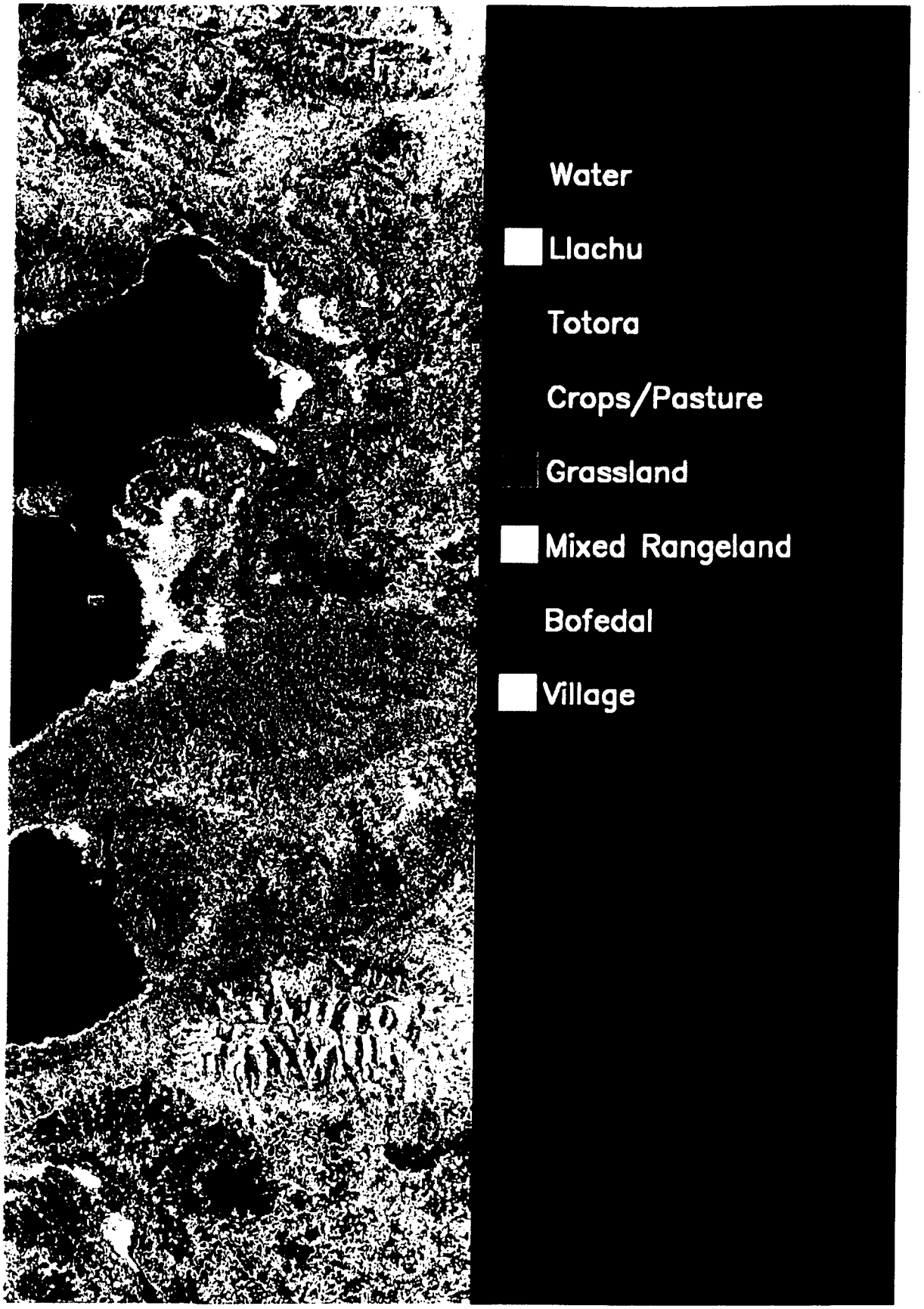
Water
Llachu
Totora
Crops/Pasture
Grassland
Mixed Rangeland
Bofedal
Village

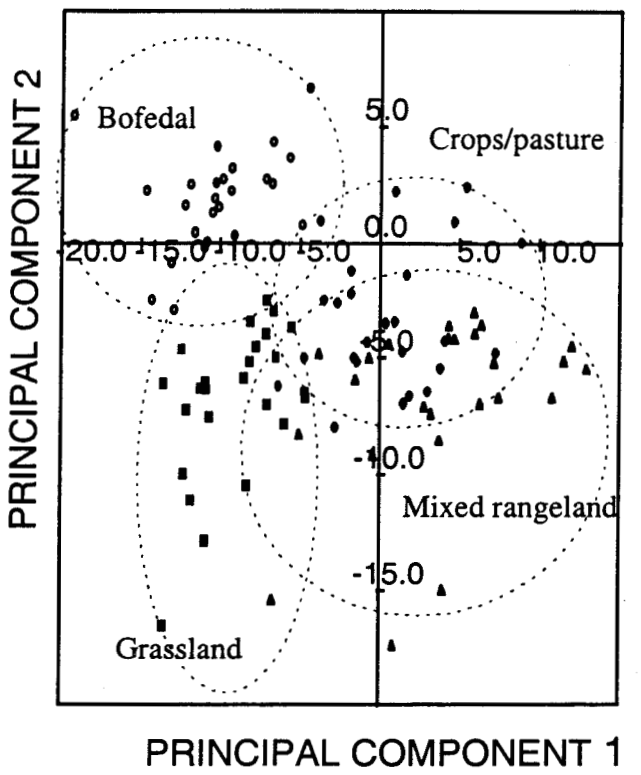
PRINCIPAL COMPONENT 2
Bofedal
Crops/pasture
Mixed rangeland
Grassland
5.0
0.0
-10.0
-15.0
-20.0
-15.0
-10.0
-5.0
5.0
10.0
PRINCIPAL COMPONENT 1

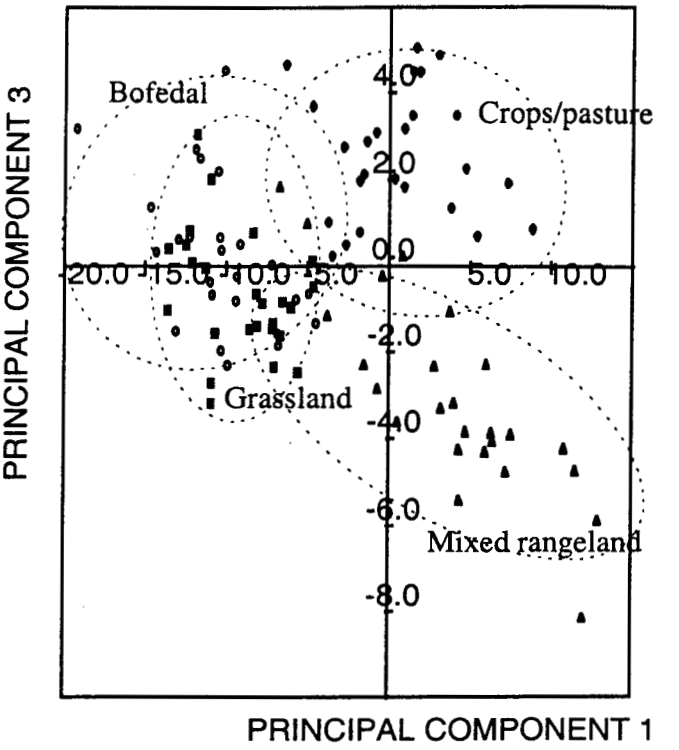
PRINCIPAL COMPONENT 3
Bofedal
Crops/pasture
Grassland
Mixed rangeland
4.0
2.0
0.0
-2.0
-4.0
-6.0
-8.0
-20.0
-15.0
-10.0
-5.0
5.0
10.0
PRINCIPAL COMPONENT 1

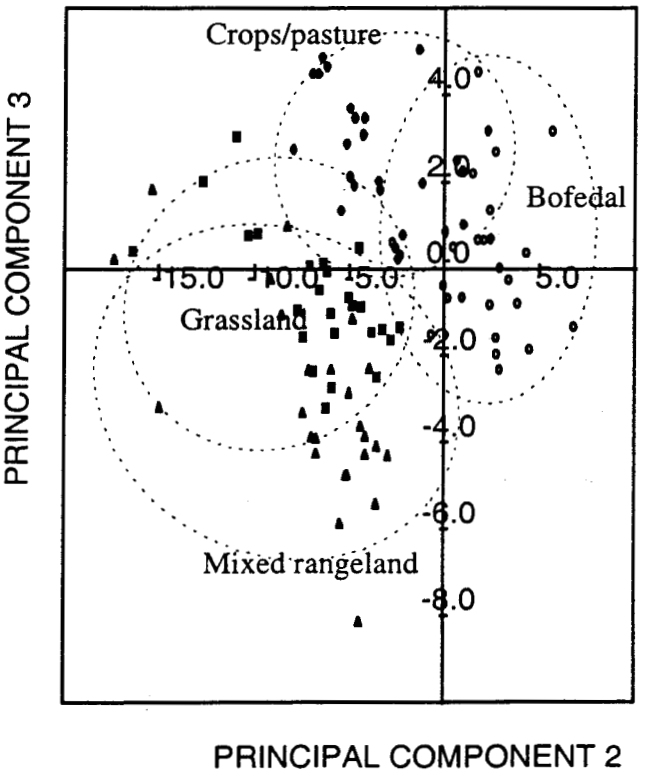
PRINCIPAL COMPONENT 3
Crops/pasture
Bofedal
Grassland
Mixed rangeland
4.0
2.0
0.0
-2.0
-4.0
-6.0
-8.0
-15.0
-10.0
-5.0
5.0
PRINCIPAL COMPONENT 2

Figure 6.